Hydrogeology Journal (2019) 27:395–407
https://doi.org/10.1007/s10040-018-1862-7

PAPER

Characterization of spatially variable riverbed hydraulic conductivity using electrical resistivity tomography and induced polarization

Sien Benoit[1] · Gert Ghysels[2] · Kevin Gommers[1] · Thomas Hermans[3] · Frederic Nguyen[4,5] · Marijke Huysmans[1,2]

Received: 19 February 2018 / Accepted: 23 August 2018 / Published online: 6 September 2018

Abstract

The spatial distribution of hydraulic conductivity (K) in riverbeds is essential to understand and model river–groundwater interactions. However, K in riverbeds varies over several orders of magnitude and its spatial distribution is closely linked to complex geological and fluvial processes. Investigating the local distribution and spatial heterogeneity of K is therefore a challenging task. The use of direct current (DC) and time-domain-induced polarization (IP) geoelectrical methods to map qualitatively the spatial distribution of K within riverbeds is described. The approach is demonstrated for a test site situated in a typical lowland river in Belgium. Inverted geophysical parameters (resistivity, chargeability and normalized chargeability) are compared with estimates of K obtained through slug tests. In general, high values of K are observed in the middle of the river and lower values towards the banks, while the opposite is true for chargeability and normalized chargeability. Therefore, there exists an inverse correlation between K and IP geophysical parameters. Furthermore, geostatistical analyses using variograms show that all parameters have ranges of similar magnitudes. The strong correlation between K and chargeability or normalized chargeability can be explained by the fact that all three parameters are mainly controlled by clay and organic matter content.

Keywords Riverbed hydraulic conductivity · Geoelectrical methods · Geostatistics · Groundwater/surface-water relations Heterogeneity

Introduction

Hydraulic conductivity is a very important, though very variable, parameter in hydrogeology, not only on a large scale, but also on a smaller scale such as in riverbeds. In riverbed sediments, it ranges mostly between 10^{-7} and 10^{-3} m/s (Calver 2001) and determines, together with the local hydraulic gradient, water exchange fluxes between the river and groundwater. River–groundwater interaction receives more and more attention in current hydrological research (Brunner et al. 2017) due to its acknowledged key role in stream ecology or biogeochemical processes (Genereux et al. 2008; Kalbus et al. 2009; Anibas et al. 2011; Sebok et al. 2014; Ghysels et al. 2018). Therefore, riverbed spatial heterogeneity of hydraulic conductivity is of special interest. In this context, this paper investigates whether geophysical measurements are informative for characterization of the hydraulic conductivity of riverbed sediments.

In recent years, research has been performed on the usefulness of geophysical methods on rivers. Electrical and electromagnetic methods have already been applied on large sea or lake surfaces for a long time (Loke and Lane 2004; Edwards 2005), but environmental applications of these methods on small-scale water surfaces such as small streams, have only recently been investigated. Crook et al. (2008) described different configurations that can be used with electrical resistivity tomography (ERT) on stream surfaces: electrodes can be floating on the water surface, submerged within the water column or physically embedded in the riverbed. Similarly for land surveys, data inversion is required after data acquisition. In

✉ Sien Benoit
sien.benoit@ugent.be

[1] Department of Earth and Environmental Sciences, KU Leuven, Celestijnenlaan 200E, 3001 Leuven, Belgium

[2] Department of Hydrology and Hydraulic Engineering, Vrije Universiteit Brussel, Pleinlaan 2, 1050 Brussels, Belgium

[3] Department of Geology, Ghent University, Krijgslaan 281, S8, 9000 Ghent, Belgium

[4] Department of Civil Engineering, KU Leuven, Kasteelpark Arenberg 40, box 2448, 3001 Leuven, Belgium

[5] Department of Urban & Environmental Engineering, University of Liège, Quartier Polytech 1 - B52, Allée de la Découverte 9, 4000 Liège, Belgium

river surveys, a significant part of the current is flowing through the water layer; therefore, the depth of investigation index (DOI) or sensitivity analyses provide essential information about the effective depth of penetration, which is required for data interpretation and error analysis (Oldenburg and Li 1999; Spitzer 1998).

As opposed to conventional measurements of hydrogeological parameters, geophysical methods are noninvasive, which avoids coring or destructive drilling in the riverbed (Clifford and Binley 2010). In addition, geoelectrical methods provide a continuous image of the subsurface instead of point measurements which are often not spaced densely enough to catch the complete spatial or temporal variability of the parameter of interest (Crook et al. 2008). However, geophysical measurements provide only indirect information on the parameter, which results in the need for petrophysical relationships for interpretation. Although the general trend and conceptual understanding of the relationship might be universal, most petrophysical relationships must be tuned due to site-specific conditions. Deriving a petrophysical relationship generally requires co-located measurements (Gottschalk et al. 2017) and, therefore, the acquisition of ground truth hydraulic conductivity. To obtain estimations of hydraulic conductivity, slug tests can be performed. A slug test is a simple, quick and inexpensive technique, and the most common method for in situ estimation of hydraulic conductivity in shallow, often unconfined formations (Butler 1998).

The relation between geophysical and hydrogeological properties of sediments and rocks has been the focus of several research projects throughout the last 70 years (Kazakis et al. 2016; Kelly 1977; Purvance and Andricevic 2000; Yadav and Abolfazli 1998). Indeed, a relationship is expected between hydraulic conductivity, K, and electrical conductivity, σ, since they have common behaviors: water flow and electrical current are both channelized through the interconnected pore space in sediments, and K and σ are both related to parameters which are measures of interconnected pore volume and interconnected pore space (Revil and Cathles 1999; Schön 1996). Slater (2007) made a review of past research on relationships between electrical properties and hydraulic conductivity. Despite the similarities between K and σ, he stated that there exists no direct, universal relationship due to different dependencies of these parameters to sediment properties. On the one hand, K is related to effective porosity and geometry of the pore space (Attwa and Günther 2013), whereas on the other hand, σ is related to pore volume, in other words the amount of electrolyte providing conduction, and to pore surface area properties, more specifically the electrical double layer (EDL) of clay minerals, which are important current flow paths. Through the combined effect of other parameters, σ is thus limited in K estimation and Slater (2007) suggested that IP (induced polarization) and SIP (spectral induced polarization) measurements provide better relations with K. Single frequency models for K estimation from IP measurements are proposed by Börner et al. (1996), Slater and Lesmes (2002) and Weller et al. (2015). Chargeability and normalized chargeability mainly depend on the interconnected pore surface area, a major factor controlling K. A stronger correlation is thus expected between K and IP parameters.

Previous studies have focused on the spatial variation of hydraulic conductivity in riverbeds using conventional K measurement methods (e.g. Chen et al. 2008; Sebok et al. 2014). Previous applications of ERT on rivers have been performed with the aim to characterize the riverbed and subsurface sediment geometry, not the hydraulic conductivity itself (e.g. Clifford and Binley 2010; Crook et al. 2008). Although IP properties can be relevant in groundwater/surface-water interaction studies, limited research in this field has been performed, as opposed to integration of ERT (Wojnar et al. 2013; McLachlan et al. 2017). To the authors' knowledge, a study combining both ERT and IP measurements to characterize spatial variability of hydraulic conductivity in riverbeds has not yet been published.

The main objective of this paper is to investigate whether ERT and IP are able to characterize the spatial variability of hydraulic conductivity in a riverbed and, if so, to what extent. To achieve this, significant correlations between hydraulic conductivity K and electrical resistivity (ρ) or chargeability (M) and normalized chargeability (MN) are sought. K is estimated in a direct way with slug tests. Resistivity and chargeability are measured with the geophysical methods ERT and IP, respectively, and a combination of both is used to calculate normalized chargeability. To analyze the correlation, spatial patterns, trends in scatterplots and linear models are determined in a comparative analysis of hydraulic conductivity, resistivity, chargeability and normalized chargeability. The study finds a negative correlation at the field site between hydraulic conductivity and chargeability, coherent with direct geological observations at the local scale. The outcomes of this paper can be used in groundwater/surface-water interaction studies that aim at improving groundwater models for more strategic water management.

Study area

A section in the Aa River in Flanders (Belgium) was investigated. The Aa River is a tributary of the Kleine Nete River, which flows via the Grote Nete River into the Scheldt River (Fig. 1a). It is a typical Flemish lowland river with an average stream discharge of 2.55 m^3/s (Waterinfo 2017), controlled by weirs across the river (Fig. 1a). The discharge regime is also influenced by the growth of macrophytes in summer (Bal and Meire 2009). The studied section (Fig. 1b) has a length of 25 m and a width of approximately 15 m, and the river flows from north-east to south-west and the river water depth varies between 0.20 m and 0.70 m, while the

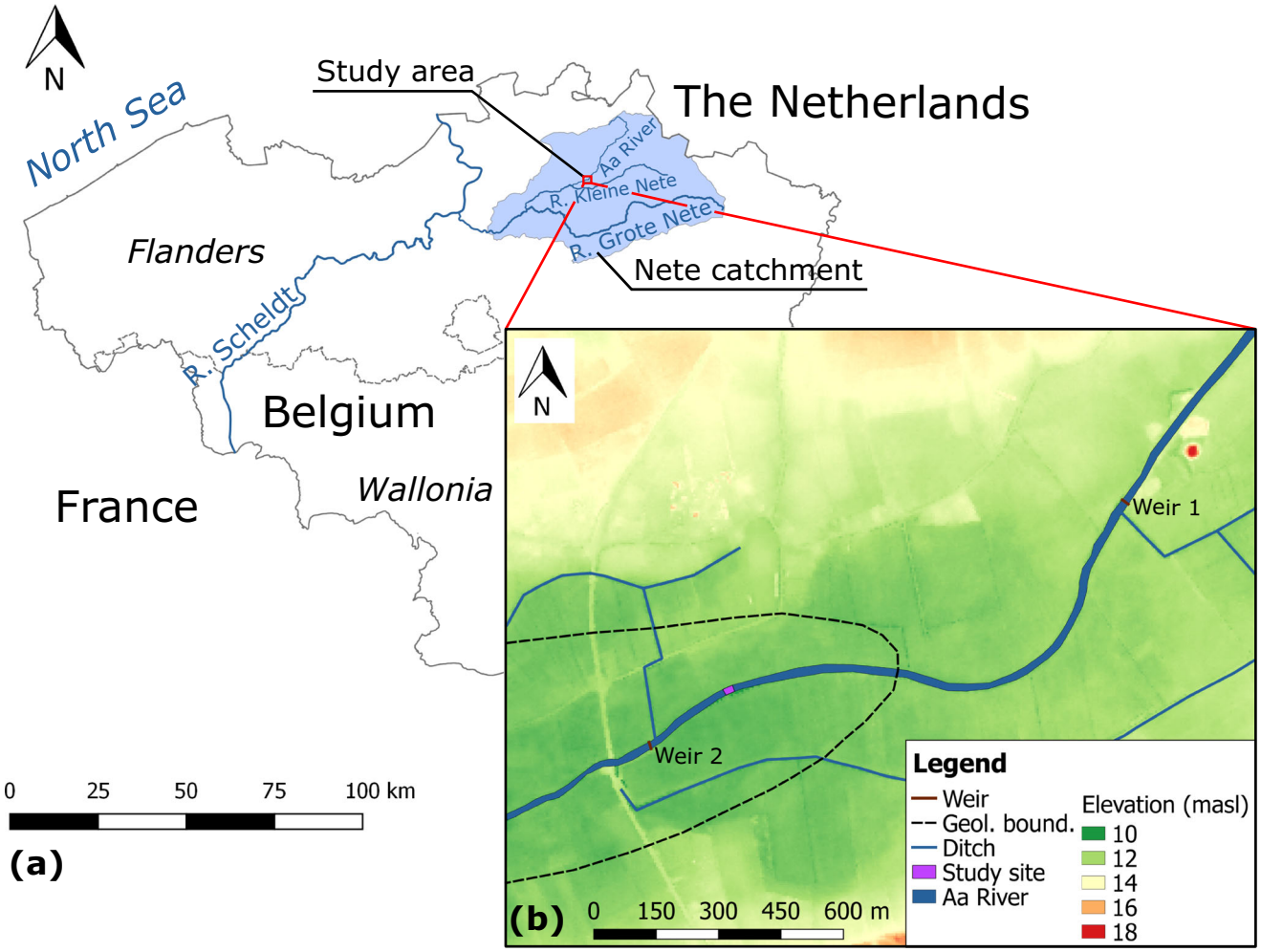

Fig. 1 Situational maps of **a** the study area in Flanders (Belgium) and **b** the river section in the Aa River. The river flows from north-east to south-west

groundwater level is shallow and occurs only 1 m below the land surface (Anibas et al. 2011).

The riverbed is mainly composed of fine sands with varying fractions of organic matter and clay. Below the riverbed sediments, Tertiary sandy deposits are present. The Kasterlee Formation, which is composed of fine sands with clay fractions, overlies the Diest Formation, which consists of heterogeneous sand with gravel layers and glauconite (DOV 2016). Together with the Berchem Formation, which lies below the Diest Formation, these geological units form an unconfined aquifer of 80 m thickness (Anibas et al. 2016).

Methods

In addition to slug tests, ERT and IP, the study used riverbed drillings to get a direct insight on the sediments. A schematic overview of the field setup for slug tests and ERT/IP measurements is shown in Fig. 2a, whereby seven profiles across the river were considered for all methods.

Riverbed drilling

Sediment cores were drilled in the riverbed with a riverbed auger to recover sediments and obtain lithological information. The auger is a hollow metal tube of 80 cm length, closed at the bottom with a valve. Eight drillings were performed, both in the middle of the river and close to the sides.

Slug tests

Slug tests were performed to obtain horizontal hydraulic conductivity (K_h) at point locations in the riverbed. It is a relatively quick, easy to implement and inexpensive method, which is most commonly used for in situ estimation of hydraulic conductivity in shallow formations (Butler 1998). By measuring the recovery of the head in a piezometer after near-instantaneous disturbance of the equivalent water level (Butler 1998; Landon et al. 2001), horizontal hydraulic conductivity can be determined. In this study, the method of Bouwer and Rice (1976) is used to calculate K_h. Moreover, repeated tests were performed to mobilize a

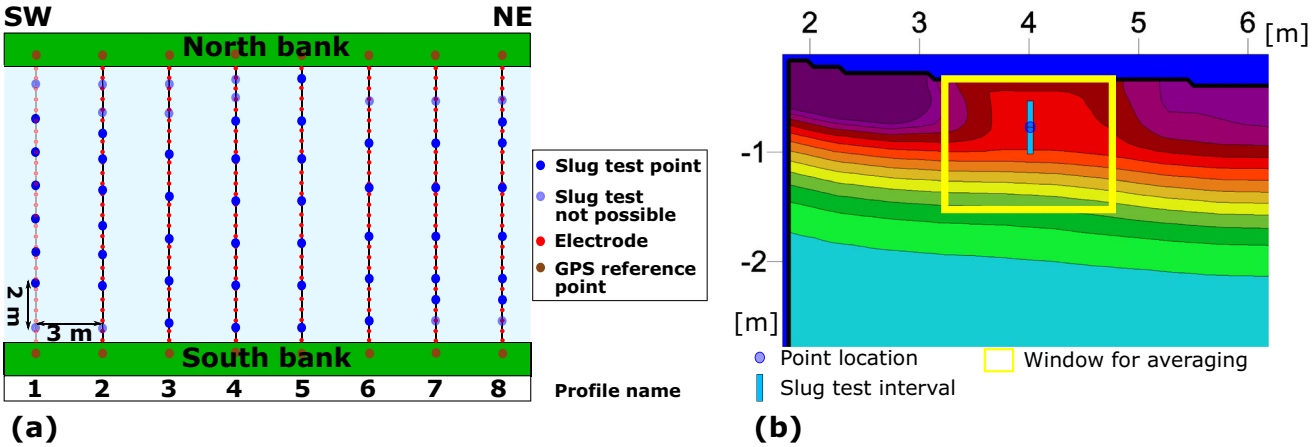

Fig. 2 **a** Field setup and linkage of the slug test survey and ERT and IP survey. Profile 1 is not measured with geophysical methods. **b** Visualization of data extraction from geoelectrical profiles

potential low K skin or at least recognize its presence (Butler 1996). The volume that is influenced by a slug test measurement in the riverbed has a height of at least 25 cm, the effective length of the screen. The lateral influence (slug test radius) is not exactly known and depends on the surrounding sediments (Butler 1998). Ramey Jr et al. (1975) indicate that a slug test radius is around the order of magnitude of 100 times the effective screen radius. In this setup, this would result in a slug test radius of approximately 1.5 m. The maximum radial extent can be estimated at 2.3 m based on the formula of Barker and Black (1983) and assumed values from Batu (1998). However, these estimations contain a lot of uncertainty, mainly due to the lack of information about the dimensionless storage coefficient, which is an important factor influencing the slug test radius.

For both the slug test and ERT/IP survey, the same seven profiles across the river were measured, with a spacing of approximately 3 m between each profile. Slug tests were performed at six point locations per profile and at two different depth intervals (from 20 to 45 cm and from 45 to 70 cm below the riverbed elevation). The point locations are distributed regularly with a separation of 2 m. If it was not possible to measure at a specific location due to local conditions, the measurement was performed at mid-distance towards the next point of the regular grid. Reference points indicating the profiles in the field were measured with a global positioning system (GPS) during the slug test survey. An extended description of the slug tests from this study is given in Ghysels et al. (2018). From now on, 'hydraulic conductivity' or 'K' will be used to indicate horizontal hydraulic conductivity K_h, unless ambiguity occurs.

Electrical resistivity tomography (ERT) and induced polarization (IP)

Electrical resistivity tomography was used to map resistivity (ρ) of the riverbed whereas induced polarization mapped the chargeability. Chargeability is the degree to which the subsurface can store electrical charge via diffusion polarization mechanisms at mineral-grain/pore-fluid interfaces. In this context, this is usually via accumulation of local charge gradients in EDLs of clay minerals, the so-called membrane polarization (Slater 2007).

Seven profiles were measured across the river with 25–28 electrodes per profile (Fig. 2a). Electrodes were separated from each other by 0.5 m and floated on the water surface by means of foam around the cable. For each measurement, four electrodes were involved. Two electrodes injected the electrical current and two other electrodes measured the resulting potential difference. To measure resistivity, the potential difference between the receiver electrodes was measured during continuous injection. To obtain chargeability from time-domain IP, the decaying residual voltage after cut-off of the applied current was measured. In this study, the dipole-dipole configuration was applied with dipole length equal to one to four electrode spacings, and the dipole spacing equal to one to six times the dipole length. The electrode spacing was 0.5 m. The dipole-dipole configuration was chosen for its higher resolution and its ability to characterize lateral variations and to detect small-scale features.

After data acquisition, inversions were performed to estimate resistivity and chargeability models from apparent resistivity and apparent chargeability data, respectively. A nonlinear smoothness-constrained least-squares inversion technique was used to iteratively find the resistivity values of the model blocks (deGroot-Hedlin and Constable 1990; Loke et al. 2003). Rectangular model blocks were used. The thickness of the model layers increased with depth with a factor of 1.05. The thickness of the first layer was set at 34% of the minimum electrode spacing (i.e. 0.5 m). The finite element method was used for forward modelling and an isotropic constraint was assumed during inversion, which means that smoothing was assumed to be similar horizontally and vertically, which is justified in the absence of any further

information. Before inversion, outliers in the data sets were removed through quality control. More specifically, all IP decay curves were visually controlled to check for their consistency: if there were inconsistencies in how the measured potential decreases in time after the current was switched off in the IP survey, those data points were removed from the data set. An average number of 92 data points per profile was kept for inversion. Since a water survey was executed, water depths below the floating electrodes were incorporated and the measured water conductivity was fixed during inversion (29 Ωm), assuming a sharp change across the water-bottom boundary.

The depth of investigation index (DOI) was determined by means of two extra inversions of the data using background reference models with different reference resistivity values (Oldenburg and Li 1999; Caterina et al. 2013). One inversion model used a low reference resistivity of 0.1 times the average apparent resistivity of the data, and the second inversion model used a high reference resistivity of 10 times the average apparent resistivity. Areas where these inverted models are similar are well constrained by the data because, despite the enforced reference resistivity, the models converge towards a similar value. In contrast, divergent values indicate a zone poorly constrained by the data. The index describing the difference between these two models is the DOI index (Fig. 3d). The closer to 0, the more the model is constrained by the data. The closer to 1, the more the model is constrained by the reference models and, therefore, the less reliable the model is.

Chargeability (M) is closely related to resistivity, which is a function of porosity, saturation, salinity and clay content (Slater and Lesmes 2002). If a medium is very conductive, after switching off the current, the potential will fall more rapidly than in a resistive medium, even if the chargeability of the lithology is high. Consequently, the measured chargeability will be lower; therefore, chargeability can be normalized by resistivity to remove this effect, resulting in the normalized chargeability MN:

$$\mathrm{MN} = M/\rho \tag{1}$$

Geostatistics

Local measurements and spatially distributed models

To find a relation between hydraulic conductivity and geoelectrical parameters, values of both must be compared on a similar scale. On the one hand, measurements of K are local and made at distinct points in the riverbed, with a well radius of only 1.5 cm, while on the other hand, inverted geoelectrical parameter models are smoothed and continuous profiles of ρ, M and MN on a discretized grid. The direct comparison of the values of K with point values of the geoelectrical parameters in the inverted profiles would not be reasonable because of the smoothing and different representative elementary volume (REV) of the geophysical measurements.

Therefore, point data corresponding to the point locations where measurements of K were made, were extracted from the inverted geophysical profiles. This was done by using a window with a specific width above the geoelectrical profiles at the locations of the K measurements (Fig. 2b). The arithmetic average of the geoelectrical block values was calculated within the window to obtain a single value of ρ, M and MN at that location, which could then be compared to the corresponding value of K. The window was cut off at the water–riverbed interface (Fig. 2b) to avoid any influence of the water body in the calculation of equivalent ρ, M and MN values.

At each location, measurements of K were performed at two consecutive depth intervals; therefore, the average of these values was calculated. Indeed, the distance between the two measurements is too small to be resolved by geoelectrical profiles. Because low K layers have a considerable influence on vertical flow through the riverbed, the harmonic mean was considered for averaging K measurements.

Several sizes of the moving window were tested with limited influence on the results. Eventually, a window width of 1.5 m was selected. The REV of the geophysical parameters is at least 0.5 m long at the surface, because of the electrode spacing of 0.5 m. However, it increases with distance to the electrodes, and depends on the applied smoothing; besides, the REV of the slug tests is difficult to define but can be roughly estimated at 1.5–2.3 m (Ramey Jr et al. 1975; Barker and Black 1983; Batu 1998). Nevertheless, one should be aware that the measured value of K is a spatially weighted average of the hydraulic conductivity of the surrounding sediments—the further from the well the sediments are, the lower their influence on the value of K at that point location (Barker and Black 1983). A width of 1.5 m for the moving window was therefore assumed an appropriate estimation in view of both REV's. Moreover, the DOI in Fig. 3d shows that the geoelectrical models have a high confidence in the upper 3 m wherein this moving window is situated.

Variogram and kriging

Exploratory geostatistical analyses were performed for hydraulic conductivity, extracted resistivity, chargeability and normalized chargeability data. Spatial patterns were compared to each other and scatterplots and linear models were made to find a spatial relation between hydraulic conductivity and one or more geoelectrical parameters. The following geostatistical methods were used as qualitative tools to support or decline

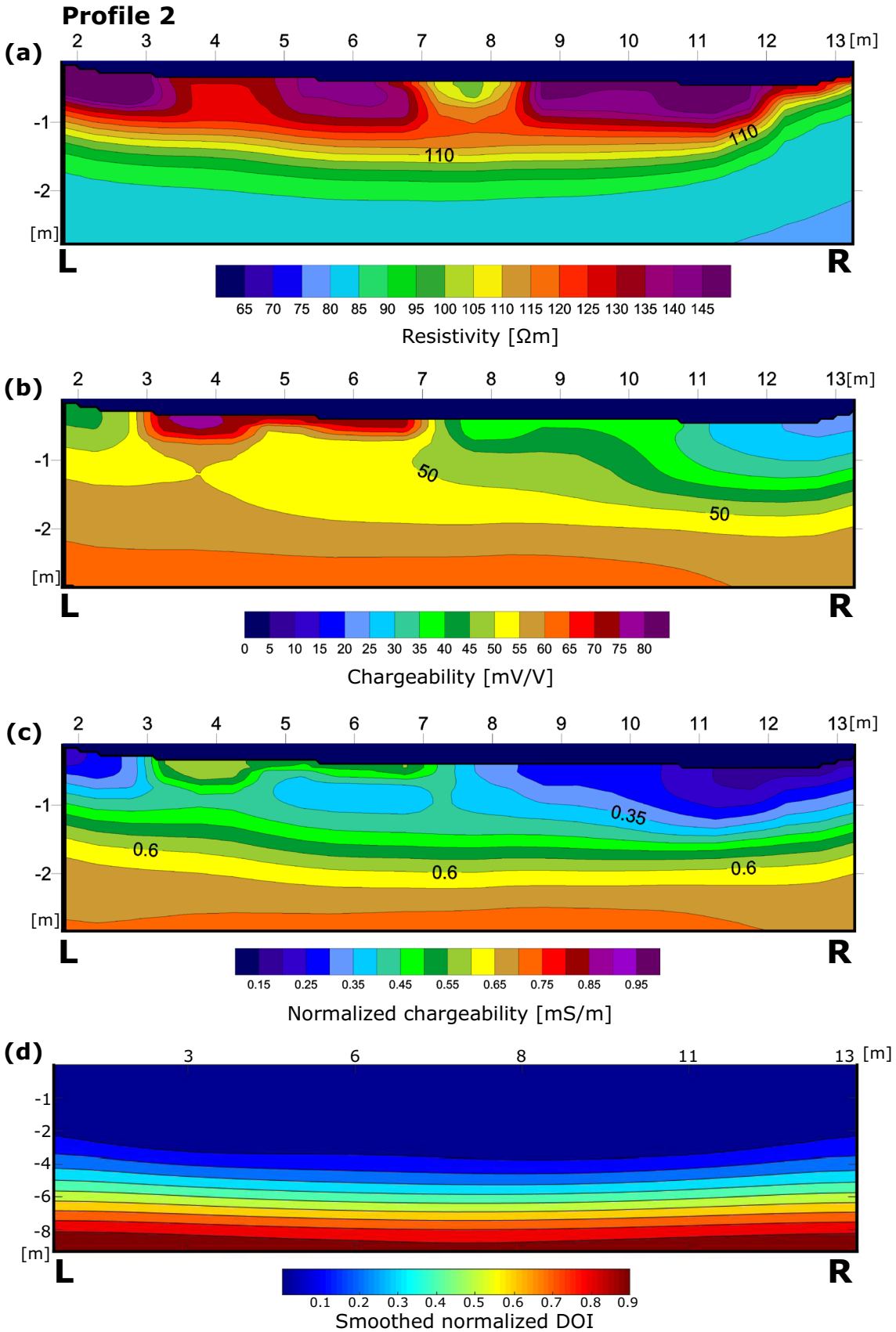

Fig. 3 Example of an inverted profile of **a** resistivity, **b** chargeability and **c** normalized chargeability. Profile (**d**) shows the depth of investigation index (DOI) of this inverted profile. It is representative for the other profiles measured across the river. *L* and *R* indicate the left and right bank respectively

the hypothesis of correlation between hydraulic conductivity and geoelectrical parameters in the riverbed.

First, omnidirectional variograms were computed using SGeMS (Remy 2004):

$$\gamma(h) = \frac{1}{2N(h)} \sum_{i=1}^{N(h)} [Z(x_i) - Z(x_i + h)]^2 \quad (2)$$

where h is the lag distance between two points, $N(h)$ is the number of pairs of measurements distant by h and Z the parameter of interest (Gelhar 1993).

To obtain values for the range, sill and nugget effect of the variogram, a model was fitted to the experimental variogram. Model fits were based on visual inspection and trial-and-error to find a good correspondence between the data and the model. By comparing the ranges of variograms of the different variables, similarities in spatial correlation could be detected.

Using the modeled variograms, ordinary kriging was performed with SGeMS (Remy 2004) to interpolate the variables between measurement points. Ordinary kriging yields a spatially continuous image that provides another way to visually compare spatial trends of hydraulic conductivity and geoelectrical parameters, removing partly the effect of small-scale variability, different REVs and measurement errors. By kriging the data, the point data of hydraulic conductivity and the geoelectrical data, extracted from the smoothed profiles, were put on a par in terms of spatial smoothing and support volume. Scatterplots of the interpolated data were generated as a qualitative tool to check the hypothesis of correlation.

Results

Lithology

Drillings in the riverbed at eight different locations and up to a depth of 50 cm revealed two types of sediment. Near the banks of the river, up to 1–1.5 m from the left bank and up to 2 m from the right bank, black, sticky fine-grained sand with a lot of organic matter and clay occurs. In the middle of the river, sediment is composed of brown, medium-to-fine-grained sand with little or no organic material or clay.

Slug tests

Measured hydraulic conductivity K of the riverbed sediments varies between 0.11 and 11.39 m/d, which shows that K ranges over two orders of magnitude in only a small area of

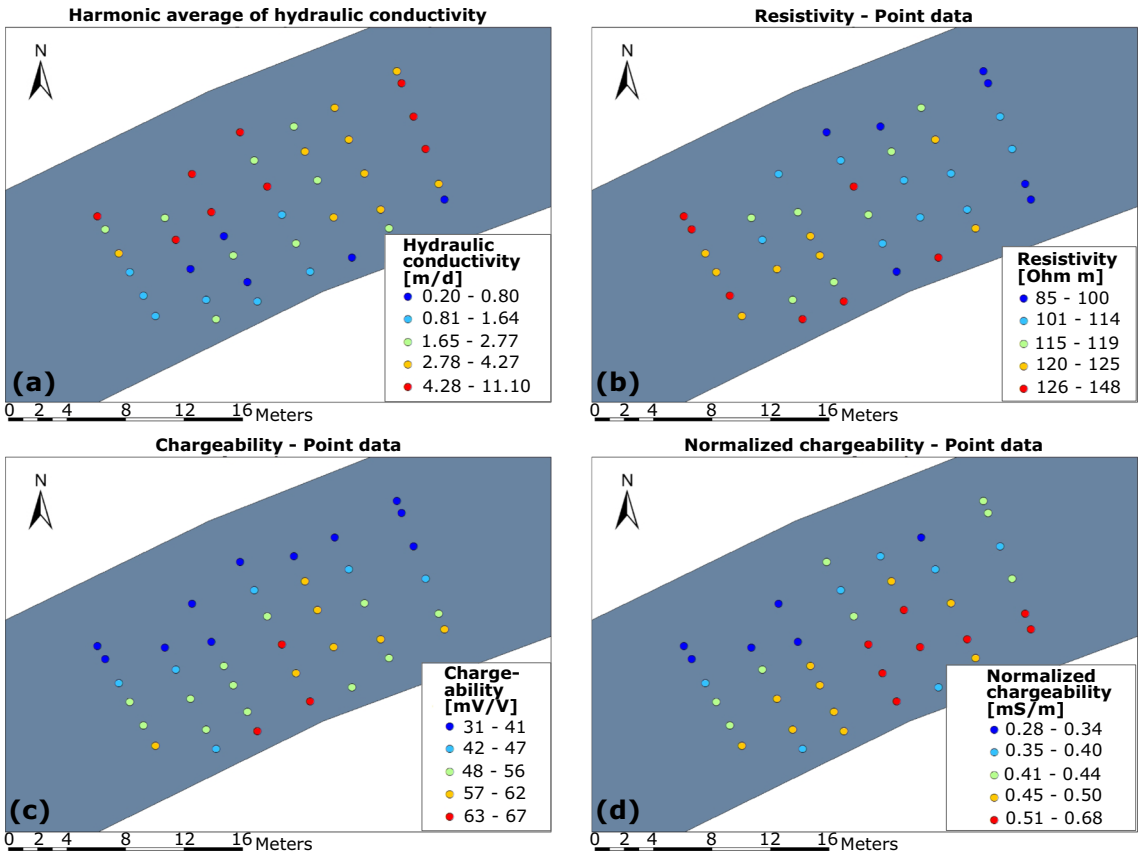

Fig. 4 Spatial distribution of point data of **a** harmonically averaged hydraulic conductivity, **b** resistivity, **c** chargeability and **d** normalized chargeability

25 × 15 m. The arithmetic average hydraulic conductivity is 4.24 m/d with a standard deviation (SD) of 3.07 m/d. An independent samples t-test indicated a significant difference between K values of the shallow and deep depth interval. For a more detailed description of results of this slug test survey, the reader is referred to Ghysels et al. (2018).

For further use, the harmonic mean of both depth intervals is considered. Spatial distribution of K (Fig. 4a) shows that hydraulic conductivity is low near the left bank with a wider band downstream in the river section. Higher values occur in the middle and towards the right half in this area. Close to the right bank, no results could be obtained because of too hard structures at shallow depth.

Electrical resistivity tomography (ERT) and induced polarization (IP)

After inversion, seven profiles across the river are obtained with continuous images of resistivity, chargeability and normalized chargeability. Resistivity in these profiles varies between 45 and 200 Ωm, chargeability varies between 0 and 85 mV/V and normalized chargeability between 0.01 and 1.00 mS/m. An example of resistivity, chargeability and normalized chargeability profiles across the river section is shown in Fig. 3a–c. The most striking features in these profiles are the decreasing resistivity and increasing chargeability and normalized chargeability with depth, which suggests increasing clay content in the sandy formations. In the shallow parts, high values of ρ, M and MN occur in the left half. In the right half, lower values occur, except for resistivity. The structures observed on this profile are also found on parallel profiles showing that the structures are elongated along the flow direction and that most heterogeneity is occurring in the perpendicular direction.

Local values of geophysical parameters are extracted from the inverted images, by averaging values within a predefined rectangle at the location of the corresponding slug test (Fig. 2b). The average of extracted resistivity is 115 Ωm with a SD of 13 Ωm. The average chargeability is 50 mV/V with a SD of 10 mV/V and the average normalized chargeability is 0.44 mS/m with a SD of 0.10 mS/m.

The spatial distribution of extracted chargeability and normalized chargeability (Fig. 4c,d) is very similar and inversely correlated with the distribution of K (Fig. 4a): the left half of the river section exposes medium to high values and in the middle and towards the right side, low values dominate. Spatial patterns of resistivity (Fig. 4b) are more difficult to identify. High values of ρ occur in the left downstream half of the section and low values in the right upstream part.

Comparison and correlation of hydraulic conductivity and geoelectrical data

Spatial patterns

Spatial patterns of hydraulic conductivity and the geoelectrical parameters are visually compared in Fig. 4. In general, an inverse correlation is present: where hydraulic conductivity is high, geoelectrical values are low and vice versa. This relation is stronger between chargeability and hydraulic conductivity. Resistivity shows less correspondence with hydraulic conductivity, although a negative relation is visible upstream and in the left half.

Scatterplots and linear regressions

Scatterplots of local hydraulic conductivity versus geoelectrical data are computed for inspection of trends in the data (Fig. 5). Decreasing trends can be recognized in all plots, and with a stronger trend observed for K vs. chargeability (Fig. 5b); however, much scatter is present.

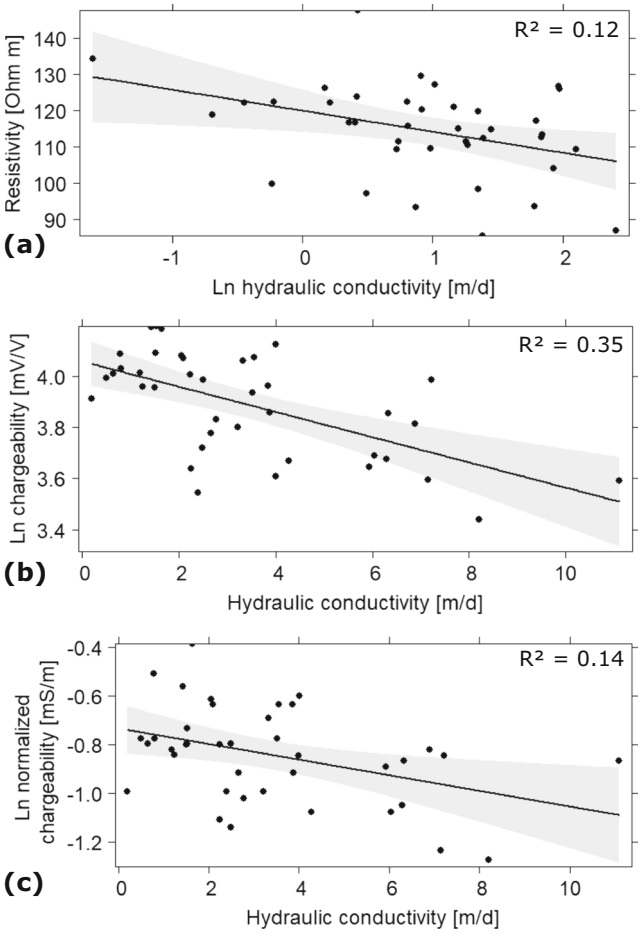

Fig. 5 Scatterplots of **a** Hydraulic conductivity vs. resistivity with linear fit. **b** Hydraulic conductivity vs. chargeability with linear fit. **c** Hydraulic conductivity vs. normalized chargeability with linear fit. *Grey bands* indicate the 95% confidence interval of the fits. Units are expressed as before logarithmic transformation, where applicable

Linear-log and log-linear regressions are fitted to these scatterplots (Fig. 5). All models are significant, but their relation is rather weak. Adjusted R^2-values are 0.12, 0.35 and 0.14 for hydraulic conductivity vs. resistivity, chargeability and normalized chargeability, respectively. Scatterplots based on ranked data and spearman correlation coefficients are calculated as well; however, these revealed similar trends and no extra information, and are therefore not discussed any further.

Variograms

Omnidirectional variograms are made for point data of harmonically averaged hydraulic conductivity, extracted resistivity, chargeability and normalized chargeability (Fig. 6). Variograms of K indicate a range of 12 m and a nugget of 2.5 $(m/d)^2$ (Fig. 6a). Ranges of resistivity, chargeability and normalized chargeability (Fig. 6b–d) are respectively 18.4, 11.5 and 11.0 m and corresponding nuggets are 50 $(\Omega m)^2$, 5 $(mV/V)^2$ and 0.002 $(mS/m)^2$ respectively.

Ranges of K, M and MN are very similar. For all three variograms, spherical models fit to the lag data, while for resistivity, a Gaussian model is more appropriate. This latter model type indicates smoothly varying data. In addition, the model for resistivity contains more uncertainty, e.g. regarding its range. The relatively large nugget effect for K indicates an effect of small-scale variability and/or measurement error, a behavior that can be expected from slug tests.

Kriging

Variograms described in the preceding section are used to interpolate point data to make continuous maps of the parameters (Fig. 7). If a nugget effect is present, ordinary kriging has an averaging effect on the resulting interpolation which removes part of the small-scale variability. The inverse correlation between hydraulic conductivity and chargeability, as well as normalized chargeability, is clearly visible (Fig. 7a,c,d). The studied river section can be roughly separated in two, with low values of hydraulic conductivity and high values of M and MN along the left side of the river changing to high values of K with low values of M and MN along the right side. In profile 6, there is an indentation in the zonation, which is visible in all three kriged maps; however, no sample is available close to the right bank, so one must be more careful with the interpretation regarding this zone. The correspondence between the interpolated maps of resistivity and

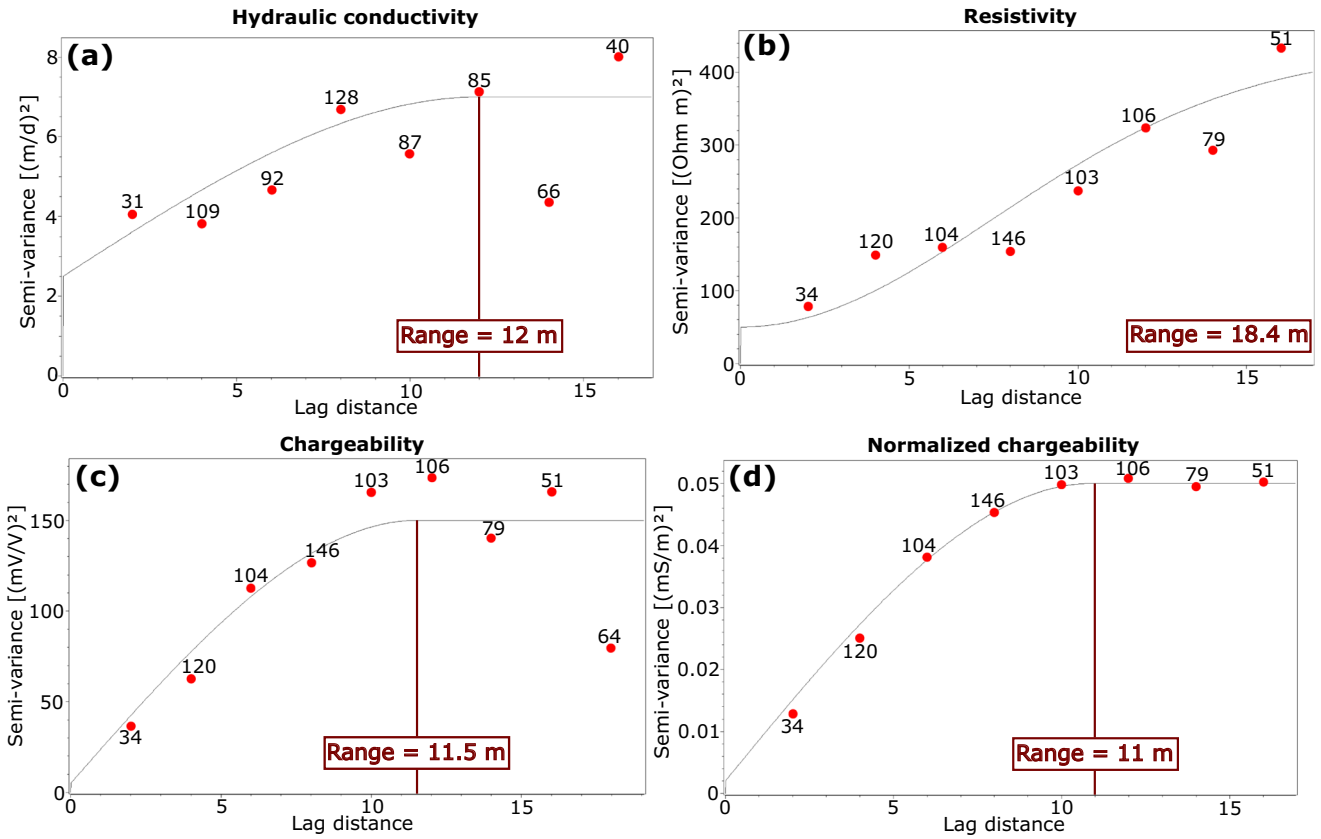

Fig. 6 Omnidirectional variograms of **a** harmonically averaged hydraulic conductivity data, **b** resistivity data, **c** chargeability data and **d** logarithmically transformed normalized chargeability data

hydraulic conductivity is less clear (Fig. 7a,b)—globally, resistivity values are high along the left bank and downstream, and decrease upstream and to the right.

To verify this visual comparison of interpolated maps, scatterplots of the interpolated data are made for hydraulic conductivity versus the geoelectrical properties (Fig. 8). To do this, only interpolated data within the investigated river section are compared, due to the fact that data outside of this area contains increasing uncertainty with distance from the measurement points. Overall, these scatterplots yield decreasing trends with significant linear regressions. The negative trend for chargeability against hydraulic conductivity data is the most significant and the most clearly visible; however, for K values between 3.5 and 4.5 m/d, there is a large range of M values. This exceptional range is larger in the plot of kriged values of resistivity and K, whereas a decreasing trend is also present in the plot of MN versus K (after kriging), but with an overall wide scatter around the fit.

Discussion

From the adjusted R^2-values of the linear models fitted to the scatterplots in Fig. 5, the correlation between K and chargeability is found to be the strongest compared to the other expected relations. Inverse correlation between hydraulic conductivity and the geoelectrical parameters under consideration can be explained by different factors. Mainly pore volume and connectivity and clay content play an important role. First of all, a well-connected pore network has a positive influence on hydraulic conductivity (Attwa and Günther 2013), whereas on the other hand, it decreases chargeability and resistivity (Slater and Lesmes 2002). This is because higher pore volume increases the amount of water present in the medium. More water in the pores increases the electrical conductivity of the sediment, and consequently decreases resistivity (Archie 1942). In addition, as water is not chargeable, a higher water content decreases the chargeability of the medium (Slater and Lesmes 2002). Clay and organic matter contents decrease hydraulic conductivity and because of their EDL, they tend to increase chargeability and normalized chargeability (Slater and Lesmes 2002). In clay-rich sediments, resistivity will decrease because of the increased electrical conductivity due to this EDL (Slater 2007; Purvance and Andricevic 2000). On the other hand, clay can decrease pore connectivity, and can therefore increase resistivity, chargeability and normalized chargeability (Slater and Lesmes 2002). This effect of decreased pore connectivity is dominant in sandy sediments (Purvance and Andricevic 2000). In media

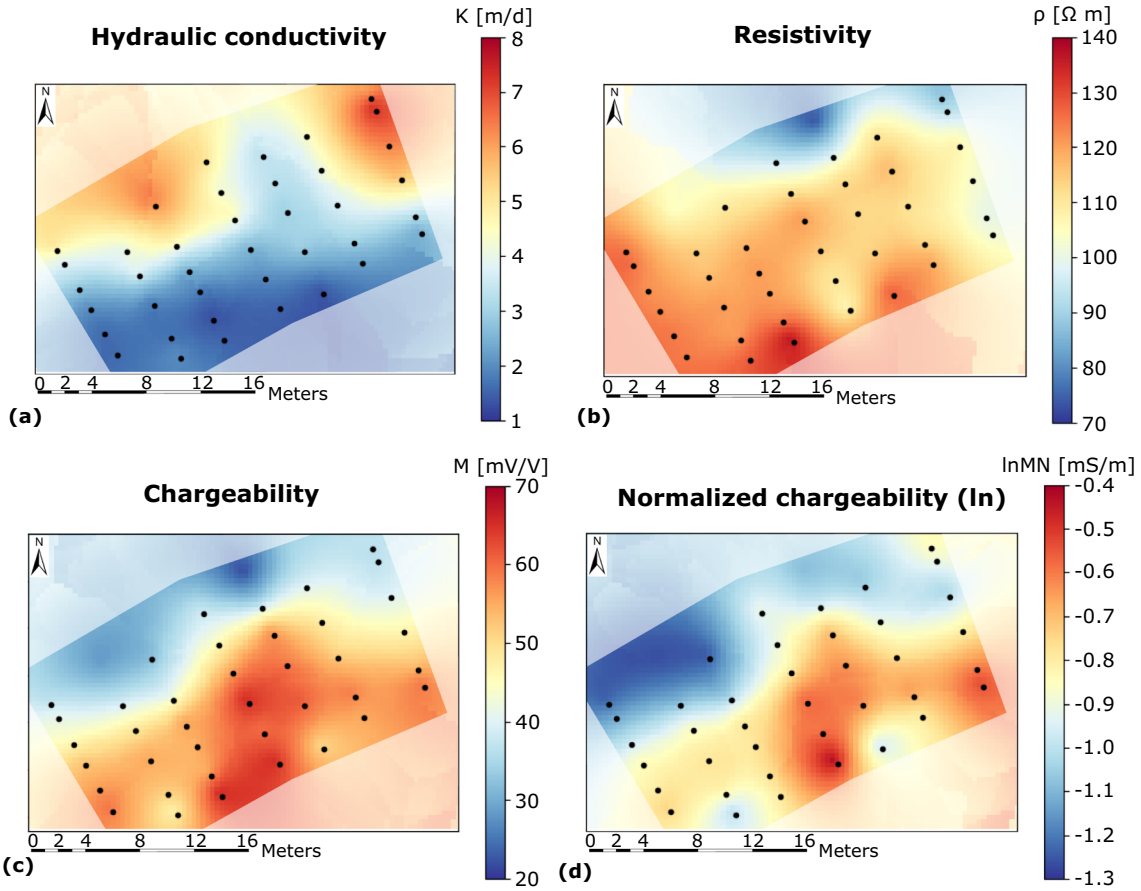

Fig. 7 Maps interpolated with ordinary kriging of **a** hydraulic conductivity, **b** resistivity, **c** chargeability and **d** logarithmic normalized chargeability

where clay is dominant, this double effect of clay is in the same direction for chargeability and normalized chargeability, but in the opposite direction for resistivity (Purvance and Andricevic 2000). Consequently, compensation of these effects can occur in resistivity profiles in clay-rich regions.

Considering these explanations and local conditions, it can be understood why hydraulic conductivity and chargeability are more correlated than normalized chargeability and why the relationship with resistivity is more complex. Sticky sands with a lot of organic matter and clay observed along the borders correspond to low hydraulic conductivity and high chargeability or normalized chargeability. Resistivity is high because the riverbed is mainly composed of sand, intermingled with other material. In the middle of the river, the organic matter and clay content is much smaller in the sandy bed, and consequently this area shows higher values of K and lower values of chargeability and normalized

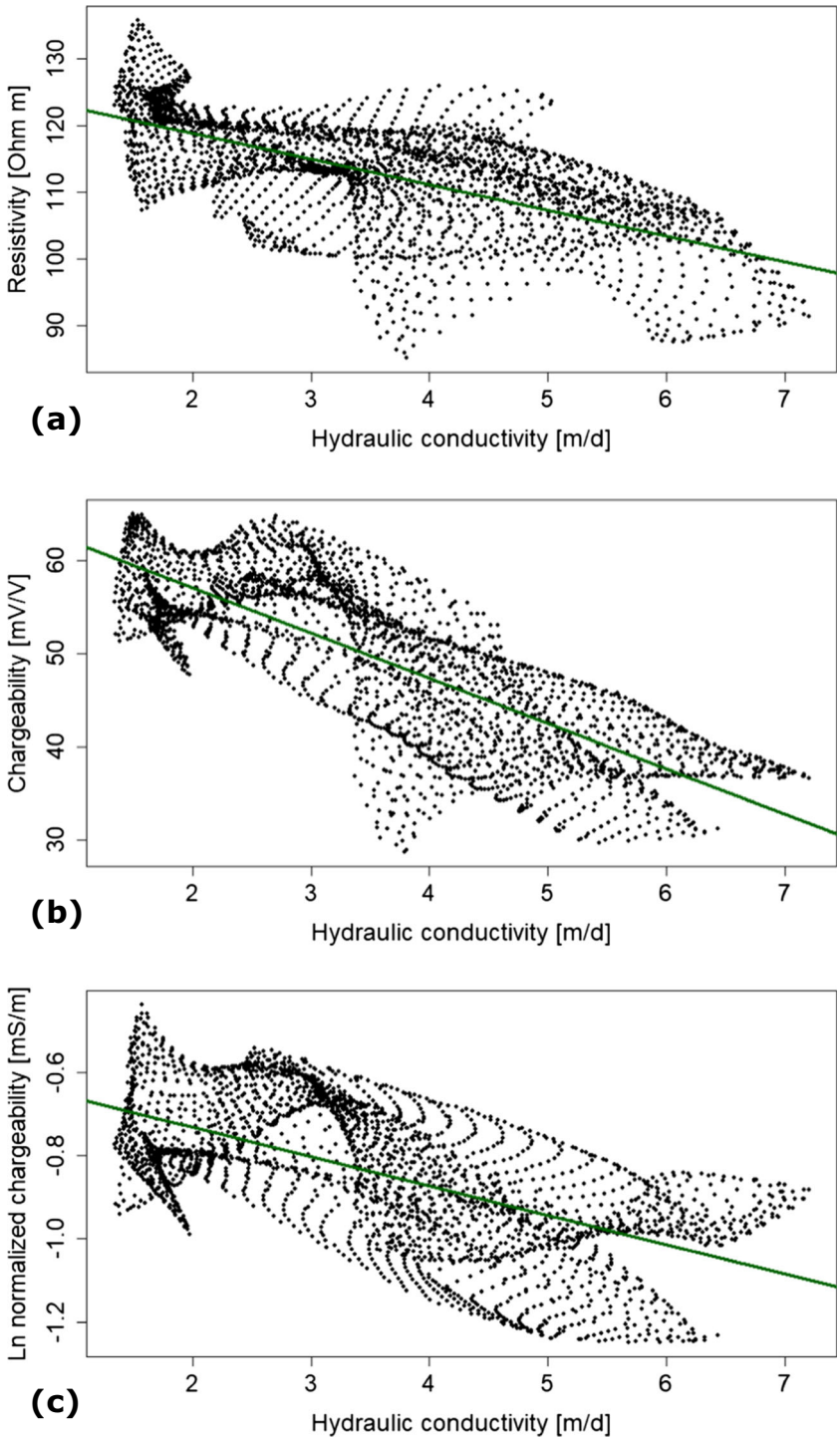

Fig. 8 Scatterplots and estimated linear fits of data from kriging maps. Hydraulic conductivity vs. **a** resistivity, **b** chargeability and **c** logarithmic normalized chargeability

chargeability. The slightly wider zone of low K values and high M values along the left bank compared to the right bank can be explained by the occurrence of the field site in a weak meander. The left bank is situated in the inner bend, where flow velocity is lower and deposition of fine particles is slightly more abundant.

Correlation between hydraulic conductivity and chargeability is however semi-quantitative. Linear models include too much scatter to be applied as a quantitative tool, but are sufficient to delineate zones of occurrence of high and low hydraulic conductivity. This is because ERT and IP are integrative methods, from which the results are smoothed by inversion, while slug test measurements are local. There is a difference in the representative elementary volumes of the slug tests and ERT/IP survey, and a perfect correlation between both cannot be expected. Slug tests measure over a depth interval of 25 cm and have an influencing radius which is not exactly known, but in comparison with ERT and IP measurements, the influential area of one slug test is small. This is because the ERT and IP survey is performed with a unit electrode spacing of 0.5 m. For points situated further away from the electrodes, the influential volume increases and the resolution decreases (Fig. 3d). In addition, during inversion, a smoothing constraint is applied (deGroot-Hedlin and Constable 1990; Loke et al. 2003). It has been shown that other constraints such as a covariance matrix (Hermans and Irving 2017) or incorporation of prior information such as structure (Caterina et al. 2014) can improve imaging of subsurface parameters.

The nugget effect that is present in the variogram of the hydraulic conductivity likely indicates small-scale variability of this variable in the riverbed. In an attempt to compensate this effect, kriging maps are calculated so that local data of hydraulic conductivity are smoothed by kriging, similar as geoelectrical data are smoothed by inversion, which yields a clearer spatial correspondence between K and M, MN and ρ. In addition, the scatterplots after kriging are a confirmation of the decreasing trend between the parameters. They also confirm that the observed trend is only qualitatively applicable, as scatter is sometimes widely present around the linear fit, especially in the intermediate ranges of K. Besides, the alignment of groups of points in the graphs are the result of gridding and smoothing when kriging (Doetsch et al. 2010). Measured points determine the shape of those groups. A few individual measurements which do not fit well in the decreasing trend consequently broaden the range of the interpolated values. These outliers are mainly situated at the right border of the studied river section.

Conclusion

Heterogeneity of hydraulic conductivity in riverbeds is currently of special interest in hydrogeological research. A correct representation of riverbed heterogeneity is important for a reliable characterization of river–groundwater interaction. It is therefore important to improve our understanding of riverbed heterogeneity to increase the accuracy of groundwater models. This study characterizes the spatial heterogeneity of hydraulic conductivity (K) in the riverbed of the Aa River (Belgium) with slug tests and compare the results with electrical resistivity tomography (ERT) and induced polarization (IP).

It was observed that the strongest correlation was between hydraulic conductivity and chargeability: high values of K correspond to low values of M. This is because chargeability and hydraulic conductivity are determined by similar factors such as interconnected pore volume and clay content. The correlation between the two parameters is further supported by the analysis of their spatial correlation using variograms and kriging; however, the observed relationship is only semi-quantitative. The reason is the variability of the slug tests measurements at the small scale, in opposition to the wider support volume of ERT and IP. Therefore, it is recommended to use ERT/IP to qualitatively map zones of high hydraulic conductivity and to target sampling locations of K, rather than in a direct quantitative way or using a blind grid. Although this petrophysical relationship is likely site-specific and semi-quantitative, the underlying petrophysical considerations suppose some universality in the link between chargeability and K for materials that exhibit membrane polarization, such as clays and organic matter.

Acknowledgements This research was financially supported by a Research Grant of the Research Foundation – Flanders (FWO) on "High resolution characterization of spatially variable riverbed hydraulic conductivity for a better assessment of river–aquifer interactions". We thank Dr. Gael Dumont from Univ. of Liège for his help during the field work in setting up the river ERT/IP. We also acknowledge the two anonymous reviewers and associate editor for their constructive comments, which helped in the improvement of the manuscript.

References

Anibas C, Buis K, Verhoeven R, Meire P, Batelaan O (2011) A simple thermal mapping method for seasonal spatial patterns of groundwater–surface water interaction. J Hydrol 397:93–104. https://doi.org/10.1016/j.jhydrol.2010.11.036

Anibas C, Schneidewind U, Vandersteen G, Joris I (2016) From streambed temperature measurements to spatial–temporal flux quantification: using the LPML method to study groundwater–surface water interaction. 216(July 2015):203–216. https://doi.org/10.1002/hyp.10588

Archie GE (1942) The electrical resistivity log as an aid in determining some reservoir characteristics. Trans Am Inst Min Metall Pet Eng 146:54–62

Attwa M, Günther T (2013) Spectral induced polarization measurements for predicting the hydraulic conductivity in sandy aquifers. Hydrol Earth Syst Sci 17(10):4079–4094. https://doi.org/10.5194/hess-17-4079-2013

Bal K, Meire P (2009) The influence of macrophyte cutting on the hydraulic resistance of lowland rivers. J Aquat Plant Manag 47:65–68

Barker JA, Black JH (1983) Slug tests in fissured aquifers. Water Resour Res 19(6):1558

Batu V (1998) Aquifer hydraulics: a comprehensive guide to hydrogeologic data analysis. Wiley, New York, 727 pp

Börner FD, Schopper W, Weller A (1996) Evaluation of transport and storage properties in the soils and groundwater zone from induced polarization measurements. Geophys Prospect 44:583–601. https://doi.org/10.1111/j.1365-2478.1996.tb00167.x

Bouwer H, Rice RC (1976) A slug test for determining hydraulic conductivity of unconfined aquifers with completely or partially penetrating wells. Water Resour Res 12:423–428

Brunner P, Therrien R, Renard P, Simmons CT, Franssen HJH (2017) Advances in understanding river–groundwater interactions. Rev Geophys 55(3):818–854

Butler JJ (1996) Slug tests in site characterization: some practical considerations. Environ Geosci 3(3):154–163

Butler JJ (1998) The design, performance, and analysis of slug tests. Lewis, New York

Calver A (2001) Riverbed Permeabilities: information from pooled data. Ground Water 39(4):546–553

Caterina D, Beaujean J, Robert T, Nguyen F (2013) A comparison study of different image appraisal tools for electrical resistivity tomography. Near Surf Geophys 11(6):639–657

Caterina D, Hermans T, Nguyen F (2014) Case studies of incorporation of prior information in electrical resistivity tomography: comparison of different approaches. Near Surf Geophys 12:451–465

Chen X, Burbach M, Cheng C (2008) Electrical and hydraulic vertical variability in channel sediments and its effects on streamflow depletion due to groundwater extraction. J Hydrol 352(3-4):250–266. https://doi.org/10.1016/j.jhydrol.2008.01.004

Clifford J, Binley A (2010) Geophysical characterization of riverbed hydrostratigraphy using electrical resistance tomography. Near Surf Geophys 8(6):493–501. https://doi.org/10.3997/1873-0604.2010035

Crook N, Binley A, Knight R, Robinson DA, Zarnetske J, Haggerty R (2008) Electrical resistivity imaging of the architecture of substream sediments. 44:1–11. https://doi.org/10.1029/2008WR006968

deGroot-Hedlin C, Constable S (1990) Occam's inversion to generate smooth, two-dimensional models form magnetotelluric data. Geophysics 55:1613–1624

Doetsch J, Linde N, Coscia I, Greenhalgh SA, Green AG (2010) Zonation for 3D aquifer characterization based on joint inversions of multimethod cross hole geophysical data. Geophysics 75(6):G53–G64

DOV (2016) Databank ondergrond Vlaanderen [Database subsurface of Flanders]. https://dov.vlaanderen.be/. Accessed 1 November 2016

Edwards N (2005) Marine controlled source electromagnetics: principles, methodologies, future commercial applications. Surv Geophys 26(6):675–700

Gelhar LW (1993) Stochastic subsurface hydrology. Prentice-Hall, Old Tappan, NJ

Genereux DP, Leahy S, Mitasova H, Kennedy CD, Corbett DR (2008) Spatial and temporal variability of streambed hydraulic conductivity in West Bear Creek, North Carolina, USA. J Hydrol 358(3–4):332–353. https://doi.org/10.1016/j.jhydrol.2008.06.017

Ghysels G, Benoit S, Awol H, Jensen EP, Tolche AD, Anibas C, Huysmans M (2018) Characterization of meter-scale spatial variability of riverbed hydraulic conductivity in a low-land river (Aa River, Belgium). J Hydrol 559:1013–1027

Gottschalk I, Hermans T, Knight R, Caers J, Cameron D, Regnery J, McCray J (2017) Integrating non-colocated well and geophysical data to capture subsurface heterogeneity at an aquifer recharge and recovery site. J Hydrol 555:407–419

Hermans T, Irving J (2017) Facies discrimination with electrical resistivity tomography using a probabilistic methodology: effect of sensitivity and regularisation. Near Surf Geophys 15:13–25

Kalbus E, Schmidt C, Molson JW, Reinstorf F, Schirmer M (2009) Influence of aquifer and streambed heterogeneity on the distribution of groundwater discharge. Hydrol Earth Syst Sci 13(1):69–77

Kazakis N, Vargemezis G, Voudouris KS (2016) Estimation of hydraulic parameters in a complex porous aquifer system using geoelectrical methods. Sci Total Environ 550:742–750. https://doi.org/10.1016/j.scitotenv.2016.01.133

Kelly WE (1977) Geoelectric sounding for estimation aquifer hydraulic conductivity. Ground Water 15(6):420–425

Landon MK, Rus DL, Harvey FE, Landonj MK, Rusl DL, Harvey FE (2001) Comparison of instream methods for measuring hydraulic conductivity in sandy streambeds. Ground Water 39(6):870–885

Loke MH, Lane JH (2004) Inversion of data from electrical resistivity imaging surveys in water-covered areas. Explor Geophys 35(4):266–271

Loke MH, Acworth I, Dahlin T (2003) A comparison of smooth and blocky inversion methods in 2D electrical imaging surveys. Explor Geophys 34:182–187

McLachlan PJ, Chambers JE, Uhlemann SS, Binley A (2017) Geophysical characterisation of the groundwater–surface water interface. Adv Water Resour 109:302–319. https://doi.org/10.1016/j.advwatres.2017.09.016

Oldenburg DW, Li YG (1999) Estimating depth of investigation in dc resistivity and IP surveys. Geophysics 64(2):403–416

Purvance DT, Andricevic R (2000) On the electrical-hydraulic conductivity correlation in aquifers. Water Resour Res 36:2905–2913

Ramey HJ Jr, Agarwal RG, Martin I (1975) Analysis of "slug test" or DST flow period date. J Can Pet Technol 14:53

Remy N (2004) S-GeMS: the Stanford geostatistical modeling software: a tool for new algorithms development. Quantitat Geol Geostatist 14:865–871

Revil A, Cathles LMI (1999) Permeability of shaly sands. Water Resour Res 35(3):651–662

Schön JH (1996) Physical properties of rocks: fundamentals and principles of petrophysics. In: Handbook of geophysical exploration: seismic exploration, 18. Pergamon, Oxford, UK

Sebok E, Duque C, Engesgaard P, Boegh E (2014) Spatial variability in streambed hydraulic conductivity of contrasting stream morphologies: channel bend and straight channel. Hydrogeol J 25(5):1283–1299. https://doi.org/10.1002/hyp.10170

Slater L (2007) Near surface electrical characterization of hydraulic conductivity: from petrophysical properties to aquifer geometries—a review. Surv Geophys 28(2–3):169–197. https://doi.org/10.1007/s10712-007-9022-y

Slater LD, Lesmes D (2002) IP interpretation in environmental investigations. Geophysics 67(1):77. https://doi.org/10.1190/1.1451353

Spitzer K (1998) The three-dimensional DC sensitivity for surface and subsurface sources. Geophys J Int 134:736–746. https://doi.org/10.1046/j.1365-246x.1998.00592.x

Weller A, Slater L, Binley A, Nordsiek S, Xu S (2015) Permeability prediction based on induced polarization: insights from measurements on sandstone and unconsolidated samples spanning a wide permeability range. Geophysics 80(2):D161–D173. https://doi.org/10.1190/geo2014-0368.1

Waterinfo (2017) Waterinfo Vlaanderen [Water information Flanders]. https://www.waterinfo.be/. Accessed 1 March 2017

Wojnar AJ, Mutiti S, Levy J (2013) Assessment of geophysical surveys as a tool to estimate riverbed hydraulic conductivity. J Hydrol 482:40–56. https://doi.org/10.1016/j.jhydrol.2012.12.018

Yadav GS, Abolfazli H (1998) Geoelectrical soundings and their relationship to hydraulic parameters in semiarid regions of Jalore, northwestern India. J Appl Geophys 39:35–51